

Random-phase-approximation approach to optical and magnetic excitations in the two-dimensional multiband Hubbard model

K. Yonemitsu and A. R. Bishop

Theoretical Division, Los Alamos National Laboratory, Los Alamos, New Mexico 87545

(Received 23 October 1991)

As a convenient qualitative approach to strongly correlated electronic systems, an inhomogeneous Hartree-Fock plus random-phase approximation is applied to response functions for the two-dimensional multiband Hubbard model for cuprate superconductors. A comparison of the results with those obtained by exact diagonalization by Wagner, Hanke, and Scalapino [Phys. Rev. B **43**, 10517 (1991)] shows that overall structures in optical and magnetic particle-hole excitation spectra are well reproduced by this method. This approach is computationally simple, retains conceptual clarity, and can be calibrated by comparison with exact results on small systems. Most importantly, it is easily extended to larger systems and straightforward to incorporate additional terms in the Hamiltonian, such as electron-phonon interactions, which may play a crucial role in high-temperature superconductivity.

I. INTRODUCTION

Physical properties of highly correlated electronic materials have been investigated with the use of a great number of different analytic and numerical techniques. Cuprate oxide superconductors are one of the most important examples of such many-body systems. Rigorous information has been obtained, by exact diagonalization and quantum Monte Carlo simulation studies, on rather small systems with a limited number of specific representative interactions. But really important physical properties might be missed in rigorous studies of such limited model systems. On the other hand, theoretical treatments should not be too approximate if properties relevant to interesting phenomena such as high-temperature superconductivity are to be captured.

To reconcile these constraints, we have proposed use of the random-phase approximation (RPA) on the basis of fully unrestricted Hartree-Fock (HF) states,¹ as a convenient and flexible qualitative technique, which can explore the influence of many physical ingredients and parameter values. The purpose of this paper is to demonstrate that this approach indeed captures qualitative features of the two-dimensional (2D), multiband Hubbard model for cuprate oxide superconductors, by comparing with results obtained recently by exact diagonalization of a 2×2 system (Wagner, Hanke, and Scalapino²). We also note some important properties that can be missed in the studies of such small systems.

In our approach, self-consistency between one-body and two-body Green's functions is not imposed in contrast to the so-called conserving approximations.³ One-body Green's functions are given in the fully unrestricted HFA. Two-body Green's functions are then obtained in the RPA, which take all linear fluctuations around the HF state into account. To recover the self-consistency, the resultant two-body Green's functions should be used to obtain new one-body Green's functions. The latter are then used to obtain new two-body Green's functions, and so on, to convergence. However, it should be stressed

that qualitative features in particle-hole excitation spectra are available even within the RPA, if linear fluctuations are studied *around true HF states*. The *true* HF states are obtained without any assumption on the form of charge and spin densities, so that they are in general spatially *inhomogeneous*.

II. HARTREE-FOCK STATES

We study the 2D multiband Hubbard model,

$$H = + \sum_{i \neq j, \alpha} t_{ij} c_{i\alpha}^\dagger c_{j\alpha} + \sum_{i, \alpha} e_i c_{i\alpha}^\dagger c_{i\alpha} + \sum_i U_i c_{i\uparrow}^\dagger c_{i\downarrow}^\dagger c_{i\downarrow} c_{i\uparrow} + \sum_{\langle i \neq j \rangle, \alpha, \beta} U_{ij} c_{i\alpha}^\dagger c_{j\beta}^\dagger c_{j\beta} c_{i\alpha}. \quad (1)$$

The operator $c_{i\alpha}^\dagger$ creates a *hole* with spin α in the Cu $d_{x^2-y^2}$ or the O $p_{x,y}$ orbital. Hopping integrals t_{ij} include the nearest-neighbor Cu-O and O-O hoppings, t_{pd} and $-t_{pp}$, respectively. On-site energies e_i contain ε_d and ε_p for the Cu and O orbitals, respectively, with $\Delta = \varepsilon_p - \varepsilon_d$. One-site repulsions U_i include U_d and U_p . Long-range repulsions U_{ij} contain a nearest-neighbor Cu-O repulsion U_{pd} . The bracket under the summation symbol means that each combination of i and j is counted once. We show results of undoped, one-hole doped, and two-hole doped systems in the case of $t_{pd} = 1$, $t_{pp} = 0$, $\Delta = 2$, $U_d = 6$, $U_p = 3$, and $U_{pd} = 1$ in the 2×2 unit-cell system with periodic boundary condition, so that comparison with exact numerical results² can be made.

As a first step, the unrestricted HF Hamiltonian is solved with self-consistency conditions for on-site and nearest-neighbor, charge and spin densities, without assumption on the form of these densities. The charge and spin densities are shown in Fig. 1 in the one-hole doped system, as an example. The radius of a circle represents charge density at that site. An arrow indicates magnitude and direction of spin density, normalized so as to touch the circle internally only if completely polarized.

In the parameters used in Ref. 2 and here, the one-hole

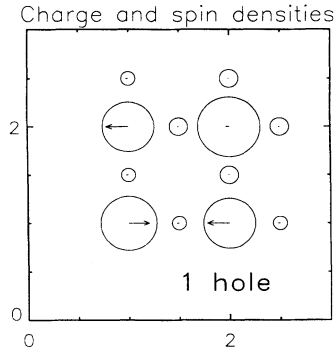


FIG. 1. Charge and spin densities in the one-hole doped 2×2 system with $\Delta=2$, $U_{pd}=1$, $U_d=6$, and $U_p=3$. The densities are represented by radii and arrows, respectively.

doped HF state contains a local charge bag, for which an added hole enters mainly a Cu site and the four surrounding O sites canceling the spin density at the central Cu site. Thus the local charge bag has $S^z=0$, but does not necessarily have $S=0$ due to intrinsic limitations of the HF states. The local charge bag is regarded as the best single-Slater-determinant state representing the Zhang-Rice singlet state.⁴

The spectral weight for single-particle excitations is given by the imaginary part of the one-body Green's function. This is shown in Fig. 2 in the undoped and the one-hole doped systems. The solid and dashed lines denote the Cu and O density of states (DOS), respectively. The O DOS was averaged over the two O positions. The energy $\omega=0$ is set at the center of the energies of the lowest unoccupied and the highest occupied orbitals in

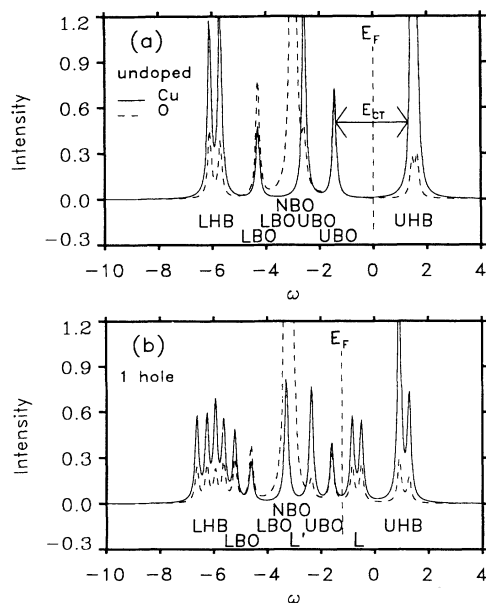


FIG. 2. Spectral weight (in arbitrary units) for single-particle excitations in the (a) undoped and (b) one-hole doped 2×2 systems with $\Delta=2$, $U_{pd}=1$, $U_d=6$, and $U_p=3$. The solid and dashed lines denote the Cu and O DOS, respectively.

the undoped system. In order to make comparison with other results² and experimental data easier, the energy scale is reversed so that the regions $\omega > E_F$ and $\omega < E_F$ correspond to creation and annihilation of an electron, respectively. However, whether a HF orbital is occupied or unoccupied is still indicated using the hole description.

In the undoped system, there are generally six bands because three states per spin per unit cell are doubled by the antiferromagnetic (AF) spin configuration. When the direct O-O hopping t_{pp} is absent, two of them form a dispersionless nonbonding oxygen band (NBO). Among the remaining four bands, two bands are well separated above and below from the NBO, and they have weight mainly at Cu sites. In electron language, these bands well below and above the NBO are called the upper Hubbard band (UHB) and the lower Hubbard band (LHB), respectively, following Ref. 2. The residual two bands have dispersions above and below but near the NBO, and they have weight mainly at O sites. We call these bands below and above the NBO the upper and the lower parts of the bonding oxygen band (UBO and LBO), respectively.

It should be noted that the limited number of momentum points in the magnetic Brillouin zone of the 2×2 unit-cell system, $\mathbf{p}=(0,0)$ and $(\pi,0)$, span these "bands." Furthermore, the LBO is degenerate with the NBO at $\mathbf{p}=(0,0)$, which state corresponds to a half of the LBO in this small system. Thus it is reasonable that the spectral weight for single-particle excitations consists of only several discrete peaks. The lowest unoccupied HF orbital belongs to the UBO in the "band" picture. It should be noted that the UBO has small but finite weight at Cu sites. If the description by a single Slater determinant is relaxed, the lowest unoccupied HF orbital or the upper half of the UBO might be well described by the Zhang-Rice singlet state,⁴ as discussed in Ref. 2.

The doped hole occupies an orbital of the UBO and it is self-trapped into a local charge bag, creating a band structure with two local HF orbitals (L) appearing in the charge-transfer gap, as shown in Fig. 2. These local HF orbitals (L) have strong Cu-O-hybridized character at the location of the local charge bag. They are regarded as correlated states (CS)² because reconstruction of bands is caused by many-body effects. Some orbitals in the NBO also appear localized and are denoted by L' hereafter. But it should be kept in mind that it is not really clear in this small system whether the L' are really localized or extended one. (See Sec. III.)

In short, the upper half of the UBO in the undoped system and the L in the doped systems are regarded as CS in Ref. 2. The NBO and L' correspond to the NBO there. The interpretation of the UHB and the LHB are the same. Meanwhile the LBO and the lower half of the UBO are not distinguished from the NBO in Ref. 2, but the corresponding structures are clearly seen there, too.

III. RPA EXCITATION SPECTRA

Next we use the RPA and study linear fluctuations around the (inhomogeneous) HF states by diagonalization of the boson Hamiltonian,¹

$$\begin{aligned}
H_{\text{RPA}} = & \sum_{\lambda > F > \mu} (\varepsilon_\lambda - \varepsilon_\mu) \zeta_{\lambda\mu}^\dagger \zeta_{\lambda\mu} \\
& + \sum_{\lambda\nu > F > \mu\tau} (v_{\lambda\mu\nu\tau}^* \zeta_{\lambda\mu}^\dagger \zeta_{\nu\tau} + \frac{1}{2} u_{\lambda\mu\nu\tau}^* \zeta_{\lambda\mu}^\dagger \zeta_{\nu\tau}^\dagger \\
& + \frac{1}{2} u_{\lambda\mu\nu\tau} \zeta_{\lambda\mu} \zeta_{\nu\tau}), \quad (2)
\end{aligned}$$

where the operator $\zeta_{\lambda\mu}^\dagger$ stands for creation of a particle-hole (p-h) pair, $\zeta_{\lambda\mu}^\dagger = c_{\lambda}^\dagger c_{\mu}$. Here the indices λ, ν and μ, τ denote unoccupied and occupied HF orbitals, respectively. The first term describes p-h excitations in the HFA, where ε_λ and ε_μ are the HF energy levels. The second term represents scattering of a p-h pair (v^* term), pair-creation and pair-annihilation of p-h pairs (u^* and u terms), where

$$\begin{aligned}
v_{\lambda\mu\nu\tau}^* = & \sum_i U_i [\phi_\lambda^*(i\uparrow) \phi_\nu^*(i\downarrow) - \phi_\lambda^*(i\downarrow) \phi_\nu^*(i\uparrow)] \\
& \times [\phi_\mu(i\uparrow) \phi_\nu(i\downarrow) - \phi_\mu(i\downarrow) \phi_\nu(i\uparrow)] \\
& + \sum_{\langle i \neq j \rangle, \alpha, \beta} U_{ij} [\phi_\lambda^*(i\alpha) \phi_\tau^*(j\beta) - \phi_\lambda^*(j\beta) \phi_\tau^*(i\alpha)] \\
& \times [\phi_\mu(i\alpha) \phi_\nu(j\beta) - \phi_\mu(j\beta) \phi_\nu(i\alpha)], \quad (3)
\end{aligned}$$

and $\phi_\lambda(i\alpha)$ is the HF wave function at site i and spin α . The formula for $u_{\lambda\mu\nu\tau}^*$ is given by interchanging the two indices ν and τ in that for $u_{\lambda\mu\nu\tau}^*$: $u_{\lambda\mu\nu\tau}^* = v_{\lambda\mu\tau\nu}^*$. The two-body Green's functions are directly obtained with the use of the eigenmodes, and their energies, of the boson Hamiltonian H_{RPA} .¹ We have also confirmed numerically that this RPA approach gives the same results obtained by the infinite sum of diagrams of the bubble and ladder types.

The spectral weight for particle-hole excitations is given by the imaginary part of the two-body Green's function in each channel O ,

$$\text{Im} \chi_O(\omega > 0) = \frac{\pi}{N_{\text{cell}}} \sum_{n \neq 0} |\langle 0 | \hat{O} | n \rangle|^2 \delta(\omega - \omega_n), \quad (4)$$

where $|0\rangle$ is the RPA ground state and $|n\rangle = \zeta_n^\dagger |0\rangle$ is the excited state with energy ω_n of the n th eigenmode. The number of unit cells are denoted by N_{cell} . Here we concentrate on the paramagnetic current channel $\hat{O} = \hat{j}_p^a$ ($a = x$ or y) and the transverse component of the AF Cu spin channel $\hat{O} = \hat{S}_{\text{Cu}}^\perp(Q)$. The paramagnetic current density operator is given by

$$\hat{j}_p^a = \sum_{i,j,\alpha} it_{ij} \varepsilon_{ij}^a c_{j\alpha}^\dagger c_{i\alpha},$$

where $\varepsilon_{ij} = \mathbf{j} - \mathbf{i}$. The nearest-neighbor Cu-Cu distance is set at unity here. Note that $\chi_{j_p^a}(\omega)$ has the opposite sign to the corresponding quantity in Ref. 2, and then $\text{Im} \chi_{j_p^a}(\omega)$ is equal to $\omega \sigma'_{\text{reg}}(\omega)$ there. The transverse component of the AF Cu spin density operator is given by

$$\hat{S}_{\text{Cu}}^\perp(Q) = \sum_{i \in \text{Cu}} (-1)^i \frac{1}{2} \hat{\sigma}_i^\perp,$$

where $\sigma_i = \sum_{\alpha, \beta} c_{i\alpha}^\dagger \sigma_{\alpha\beta} c_{i\beta}$, σ stands for Pauli matrices.

When the HF spin density is aligned in the x direction, the transverse component denotes one of the y and z components.

It should be noted that all the linear excitations were obtained in the RPA by diagonalization of the boson Hamiltonian H_{RPA} . Each linear excitation is investigated by looking at what kind of particle-hole excitations contribute to it, as described in our previous report.¹ Linear excitations are classified into local shape modes, "shake-off" branches of modes related to combinations of local and extended HF orbitals, and extended modes such as appear in the undoped case.

The real and regular (i.e., nonsingular) part of optical conductivity, $\sigma'_{\text{reg}}(\omega) = \text{Im} \chi_{j_p^a}(\omega)/\omega$, is shown in Fig. 3 in the undoped (solid line), one-hole doped (dashed line), and two-hole doped (dash-dotted line) systems.

In the undoped system, the main optical absorption peak at $\omega = 3.6$ is due to charge-transfer modes. The p-h pairs which contribute to them are associated with the UHB and the NBO (UHB \rightarrow NBO transition). Thus the main peak corresponds to the peak A in Fig. 12(b) of Ref. 2. The charge-transfer optical weight extends above $\omega \simeq \Delta + U_{pd} = 3$, while the energy difference between the UHB and the NBO is slightly larger than $\omega \simeq \Delta + 2U_{pd} = 4$, as observed in the exact diagonalization.² This kind of excitonic effect was discussed in the 1D extended Peierls-Hubbard model at half filling in the RPA by Nasu.⁵

In the one-hole doped system, the peaks at $\omega = 3.3, 3.7$, and 4.2 correspond to transitions UHB \rightarrow NBO, UHB $\rightarrow L'$, and UHB $\rightarrow L'$, respectively. Thus these peaks correspond to the peak A in Ref. 2. In larger systems, they might form a broad band. In addition, there appear peaks related to the local gap states (L). The peaks at $\omega = 2.4, 2.6$, and 1.8 correspond to transitions $L \rightarrow L'$, $L \rightarrow \text{NBO}$, and $L \rightarrow L'$, respectively. In other words, they represent the process in which the O hole is unbound from the Cu spin in the local charge bag. These peaks correspond to the peak B in Ref. 2. The Drude peak (D in Ref. 2) is not reproduced due to our periodic boundary condition, as in Fig. 14 of Ref. 2. (See below.)

In the two-hole doped system, the peaks at $\omega = 2.3, 3.5$, and 1.7 correspond to transitions UHB $\rightarrow L'$, UHB $\rightarrow L'$, and $L \rightarrow L'$, respectively. Here the main peak ($\omega = 2.3$) is

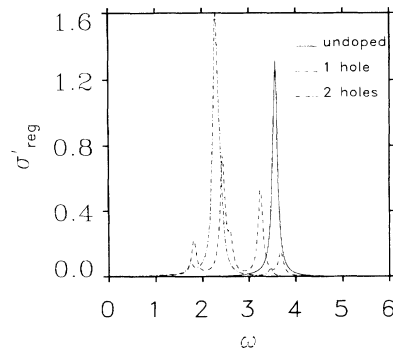


FIG. 3. Real, regular part (i.e., excluding $\omega = 0$) of optical conductivity with $\Delta = 2$, $U_{pd} = 1$, $U_d = 6$, $U_p = 3$, and periodic boundary conditions.

located slightly lower than the main peak related to the L in the one-hole doped system ($\omega=2.4$).

To clarify whether each peak is a true peak or just a part of a rather broad band, larger systems should be studied. But we emphasize here that most of the features in optical excitations observed by the exact diagonalization² are well reproduced by the much simpler technique of inhomogeneous HF plus RPA.

We have also estimated the Drude weight (the real and singular part at $\omega=0$) in the optical conductivity for the systems with periodic boundary condition,^{6,7} by calculating both the negative paramagnetic and the positive diamagnetic contributions in the RPA with the help of the Hellmann-Feynman theorem.⁸ In the half-filled 1D single-band Hubbard model, we find oscillation with increasing system size N , related to the two series of system sizes $N=4n$ and $N=4n+2$, and it converges exponentially with N , as found by exact Bethe-ansatz calculations.⁹ However, its thermodynamic limit is positive and finite in contrast to the exactly known value of zero^{2,9} expected for insulators.⁶ This is presumably due to underestimation of the paramagnetic contribution. Therefore the present approach is not quantitative enough to be used to distinguish between metals and insulators in the half-filled 1D single-band Hubbard model. Nevertheless it gives some guidance on the metal-insulator transition in the presence of doping and especially for less special models. Thus, in the 2D multiband Hubbard model, the estimated Drude weight from the RPA increases with doping for a fixed system size (2×2), which is consistent with the exact result.² In the case of $\Delta=2$, $U_{pd}=1$, $U_d=6$, and $U_p=3$ with periodic boundary condition, the Drude weight (D in the notation of Ref. 2) changes from 0.34 (undoped), 0.63 (one hole) to 1.1 (two holes).

The spectral weight for AF magnetic excitations at Cu sites $\text{Im } \chi_{s_{\text{Cu}}^{\perp}(\mathbf{Q})}(\omega)$ is shown in Fig. 4 in the undoped (solid line) and one-hole doped (dashed line) systems.

In the undoped system, the main peak is at $\omega=0$ and due to the Goldstone modes, which are related to restoration of the spin rotation symmetry. Here $\text{Im } \chi_{s_{\text{Cu}}^{\perp}(\mathbf{Q})}(\omega=0)$ is set to be zero because (for technical convenience²) the retarded Green's functions are used instead of the casual ones. In the thermodynamic limit,

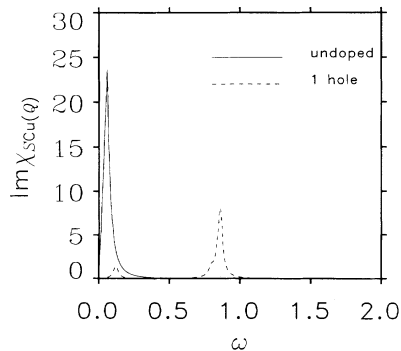


FIG. 4. Spectral weight for AF magnetic excitations at Cu sites with $\Delta=2$, $U_{pd}=1$, $U_d=6$, and $U_p=3$.

when the AF spin configuration on Cu sites has long-range order at zero temperature, spin-wave excitations are expected with dispersion extending from zero to finite energy. Meanwhile, if the ground state is nondegenerate, exact excitation spectra for finite systems generally show a finite gap which may disappear in the thermodynamic limit. We believe that the Goldstone modes obtained here belong to these spin-wave modes and should have finite energies in finite systems if the spin rotation symmetry is properly included in the RPA. Thus, the analysis of the lowest peak in this channel by the two-site quantum spin system² may be inadequate in larger systems.

In the one-hole doped system, the peak due to the Goldstone modes are largely suppressed and a new peak appears in the low-energy range. This new peak has energy 0.86 and corresponds to the transition $L \rightarrow \text{UBO}$. A strong-coupling estimate of the nearest-neighbor Cu-O Kondo exchange coupling is 0.7 and comparable to this peak energy. In the exact diagonalization, the corresponding peak is reported to have energy 1.47 and suggested to be related to local Cu-O triplet excitation from the Zhang-Rice singlet.² If this is true and were reproduced in our approach, this process would be described by the transition $L \rightarrow L'$. The reason of the discrepancy is not clear.

IV. SUMMARY

As a convenient qualitative approach to strongly correlated systems, inhomogeneous HF plus RPA (Ref. 1) has been applied to response functions in the 2D multiband Hubbard model, which has been studied extensively as a model of cuprate superconductors. Comparison of our results with those obtained on small systems by exact diagonalization by Wagner, Hanke, and Scalapino² shows that overall structures in optical and magnetic particle-hole excitation spectra are well reproduced by inhomogeneous HF plus RPA.

For example, an optical absorption peak is induced by added holes at an energy less than the charge-transfer gap, and its spectral weight increases in proportion to doping concentration. This absorption is mainly caused by transition of a hole from local gap states to the nonbonding oxygen band: in other words, unbinding of the O hole from the Cu spin in the local charge bag. The main charge-transfer peak, caused by transition of a hole from the upper Hubbard band (using the electron description) to the nonbonding oxygen band, has a reduced spectral weight as doping increases. These peak positions are similar to those obtained by the exact diagonalization.

The present approach should not in general be used to distinguish between metals and insulators because it does not treat small-wave-number low-frequency charge excitations properly and gives an incorrect thermodynamic limit of the Drude weight. However it gives a rather reasonable result as far as doping dependence is concerned: The Drude weight increases with doping as expected by optical conductivity measurements¹⁰ as well as the exact diagonalization studies.

A magnetic absorption peak is also induced by added holes at an energy comparable to a strong-coupling estimate of the nearest-neighbor Cu-O Kondo exchange coupling. A zero-energy magnetic peak of the undoped state is caused by Goldstone modes, related to restoration of the spin rotation symmetry, and is largely suppressed at $q=(\pi, \pi)$ by doping.

The advantages of our approach are that (i) major qualitative features of particle-hole excitations are well reproduced by the conceptually and computationally simple method of inhomogeneous HF plus RPA; the method can be calibrated and controlled by comparison with exact results on small systems; and (ii) it is easy to extend to

larger systems and to incorporate additional terms in the Hamiltonian such as electron-phonon interactions. Such terms may play crucial roles in high-temperature superconductivity. As will be described elsewhere,¹¹ it is also straightforward to extend the method to obtain optical conductivity spectra in both phonon-energy and charge-transfer-energy regions on the same footing.

ACKNOWLEDGMENTS

We are grateful to Dr. I. Batistić for fruitful discussions. This work was supported by the U.S. DOE.

¹K. Yonemitsu, I. Batistić, and A. R. Bishop, Phys. Rev. B **44**, 2652 (1991).

²J. Wagner, W. Hanke, and D. J. Scalapino, Phys. Rev. B **43**, 10 517 (1991).

³G. Baym and L. P. Kadanoff, Phys. Rev. **124**, 287 (1961); G. Baym, *ibid.* **127**, 1391 (1962); N. E. Bickers and D. J. Scalapino, Adv. Phys. (N.Y.) **193**, 206 (1989).

⁴F. C. Zhang and T. M. Rice, Phys. Rev. B **37**, 3759 (1988).

⁵K. Nasu, J. Phys. Soc. Jpn. **53**, 302 (1984).

⁶W. Kohn, Phys. Rev. **133**, A171 (1964).

⁷B. S. Shastry and B. Sutherland, Phys. Rev. Lett. **65**, 243 (1990); Ref. 2 and references therein.

⁸D. Baeriswyl, J. Carmelo, and A. Luther, Phys. Rev. B **33**, 7247 (1986); **34**, 8976 (E) (1986).

⁹R. M. Fye, M. J. Martins, D. J. Scalapino, J. Wagner, and W. Hanke, Phys. Rev. B **44**, 6909 (1991).

¹⁰S. Uchida, T. Ido, H. Takagi, T. Arima, Y. Tokura, and S. Tajima, Phys. Rev. B **43**, 7942 (1991).

¹¹K. Yonemitsu and A. R. Bishop (unpublished).